Supporting Information for

"*Ultra-wideline ^{14}N Solid-State NMR as a Method of Differentiating Polymorphs: Glycine as a Case Study*"

Stanislav L. Veinberg,[†] Zachary W. Friedl,[†] Kristopher J. Harris,[†] Luke A. O'Dell[‡] and Robert W. Schurko[†,]*

[†] *Department of Chemistry and Biochemistry, University of Windsor, 401 Sunset Avenue, Windsor, Ontario, Canada N9B 3P4*
[‡] *Institute for Frontier Materials, Deakin University, Waurn Ponds Campus, Geelong, Victoria Australia, 3220*

* To whom correspondence should be addressed. ; Tel: +1 519 253 3000 x3548
Fax: +1 519 973 7098; E-mail: rschurko@uwindsor.ca; Web: http://www.uwindsor.ca/schurko

Table of Contents:

Table S1. Experimental parameters for ^{14}N WURST-CPMG NMR experiments

	α-glycine	β-glycine	γ-glycine*	glycine HCl
Number of transients per sub-spectrum	256	7200	512	256
Number of sub-spectra	8	7	8	8
Transmitter frequency step (kHz)	150	150	150	150
^{14}N Recycle delay (s)	1	0.5	1	1
Experimental time (minutes)	35.5	455.4	71.1	35.5
WURST sweep range (kHz)	2000	3000	2000	2000
Number of Meiboom-Gill Loops	200	200	200	200
Acquisition points per echo	200	200	200	200
Spikelet Separation (kHz)	10	10	10	10
WURST pulse length (μs)	50	50	50	50
^{1}H decoupling power (kHz)	40	40	40	40
WURST pulse power (kHz)	28	28	28	28
Spectral window width (kHz)	2000	2000	2000	2000

* Identical experimental parameters used for acquisition of γ-glycine-ND_3^+.

Table S2. Experimental parameters for ^{14}N WURST-CPMG Variable Temperature NMR experiments of individual sub-spectra

	α-glycine	γ-glycine	glycine HCl
Transmitter Frequency (MHz)	29.175	29.175	29.325
Number of transients per sub-spectrum	512	512	128
Experimental time (minutes)	8.9	8.9	2.2
WURST sweep range (kHz)	2000	2000	2000
Recycle delay (s)	1	1	1
Number of Meiboom-Gill Loops	200	200	200
Acquisition points per echo	200	200	200
Spikelet Separation (kHz)	10	10	10
WURST pulse length (μs)	50	50	50
^{1}H decoupling power (kHz)	40	40	40
WURST pulse power (kHz)	28	28	28
Spectral window width (kHz)	2000	2000	2000
Temperature Range (°C)	−65 to 181	−43 to 136	−88 to 92

Table S3. Experimental parameters for ^{14}N WURST-QCPMG Variable Temperature NMR experiments for complete powder pattern acquisition

	α-glycine	γ-glycine
Number of transients per sub-spectrum	256	512
Number of sub-spectra	8	8
Transmitter frequency step (kHz)	150	150
^{14}N Recycle delay (s)	1	1
Experimental time (minutes)	35.5	71.1
WURST sweep range (kHz)	2000	2000
Number of Meiboom-Gill Loops	200	200
Acquisition points per echo	200	200
Spikelet Separation (kHz)	10	10
WURST pulse length (μs)	50	50
^{1}H decoupling power (kHz)	40	40
WURST pulse power (kHz)	28	28
Spectral window width (kHz)	2000	2000
Temperature (°C)	−43	92

Table S4. Experimental parameters for comparison of ^{14}N BRAIN-CP/WURST-CPMG NMR experiment versus ^{14}N WURST-CPMG NMR experiment using a sub-spectrum of glycine HCl

	BRAIN-CP/ WURST-CPMG	WURST-CPMG
Transmitter Frequency (MHz)	29.225	29.225
Number of transients per sub-spectrum	256	256
^{14}N Recycle delay (s)	–	2.5
^{1}H Recycle delay (s)	2.5	–
Experimental time (minutes)	10.8	10.8
Spectrum width (kHz)	2000	2000
Dwell time (μs)	0.5	0.5
^{1}H excitation (π/2) pulse (μs)	4.0	–
^{1}H excitation (π/2) pulse rf (kHz)	62.5	–
^{1}H Spin-lock rf power (kHz)	45	–
Contact time (ms)	10	–
CP sweep range (kHz)	400	–
WURST refocusing pulse length (μs)	50	50
WURST refocusing pulse power (kHz)	28	28
WURST refocusing sweep range (kHz)	450	460
Number of Meiboom-Gill Loops	200	200
Acquisition points per echo	200	200
CPMG echo length (per echo, μs)	100	100
Spikelet Separation (kHz)	10	10
^{1}H decoupling power (kHz)	45	45
Spectral window width (kHz)	2600	2600

Table S5. Experimental parameters for ^{14}N BRAIN-CP/WURST-CPMG NMR experiments for complete powder pattern acquisition

	glycine HCl
Number of transients per sub-spectrum	64
Number of sub-spectra	11
Transmitter frequency step (kHz)	90
^{1}H Recycle delay (s)	1
Experimental time (minutes)	11.8
Spectrum width (kHz)	2000
Dwell time (μs)	0.5
^{1}H excitation (π/2) pulse (μs)	4.0
^{1}H excitation (π/2) pulse rf (kHz)	62.5
^{1}H Spin-lock rf power (kHz)	45
Contact time (ms)	10
CP sweep range (kHz)	400
WURST refocusing pulse length (μs)	50
WURST refocusing pulse power (kHz)	28
WURST refocusing sweep range (kHz)	450
Number of Meiboom-Gill Loops	200
Acquisition points per echo	200
CPMG echo length (per echo, μs)	100
Spikelet Separation (kHz)	10
^{1}H decoupling power (kHz)	45
Spectral window width (kHz)	2600

Table S6. Atomic parameters for the four compounds under investigated. Atomic distances and angles were measured using the structures from the respective references, without optimization of the crystal structures.

Geometry parameters (no H-optimization)				
	α-glycine [53]	β-glycine [4]	γ-glycine [54]	glycine HCl [55]
C-N (Å)	1.475 (1)	1.475 (3)	1.488 (1)	1.461 (6)
$N\text{-}H_1$ (Å)	1.053 (1)	0.901 (18)	1.055 (1)	1.013 (3)
$N\text{-}H_2$ (Å)	1.036 (1)	0.884 (20)	1.054 (1)	1.037 (1)
$N\text{-}H_3$ (Å)	1.025 (1)	0.895 (25)	1.046 (1)	1.038 (1)
H_1---O (Å)	1.725 (1)	1.864 (19)	1.755 (1)	2.222 (9)
H_2---O (Å)	1.827 (1)	1.967 (30)	1.809 (1)	–
H_3---O (Å)	2.118 (1)	2.302 (24)	1.929 (1)	–
H_2---Cl (Å)	–	–	–	2.123 (2)
H_3---Cl (Å)	–	–	–	2.160 (2)
$C\text{-}N\text{-}H_1$ (°)	112.08 (1)	111.72 (125)	111.96 (1)	111.34 (1)
$C\text{-}N\text{-}H_2$ (°)	112.00 (1)	113.28 (141)	107.96 (1)	109.62 (1)
$C\text{-}N\text{-}H_3$ (°)	110.22 (1)	109.95 (147)	110.94 (1)	112.45 (1)

Table S7. Atomic parameters for the four compounds under investigated. Atomic distances and angles were measured using the structures from the respective references after geometry optimization of the proton positions.

Geometry parameters (H-optimization)				
	α-glycine [53]	β-glycine [4]	γ-glycine [54]	glycine HCl [55]
C-N (Å)	1.475	1.475	1.488	1.461
N-H_1 (Å)	1.065	1.067	1.060	1.038
N-H_2 (Å)	1.052	1.036	1.052	1.052
N-H_3 (Å)	1.038	1.053	1.042	1.052
H_1---O (Å)	1.712	1.697	1.750	2.206
H_2---O (Å)	1.812	2.201	1.806	–
H_3---O (Å)	2.112	1.802	1.933	–
H_2---Cl (Å)	–	–	–	2.106
H_3---Cl (Å)	–	–	–	2.143
C-N-H_1 (°)	112.693	111.07	112.226	111.580
C-N-H_2 (°)	112.115	110.586	107.293	109.305
C-N-H_3 (°)	110.465	111.662	110.941	112.983

Table S8. Calculated EFG tensor values

	Plane-wave DFT			Plane-wave DFT (optimized)		
	V_{11} (a.u.)	V_{22} (a.u.)	V_{33} (a.u.)	V_{11} (a.u.)	V_{22} (a.u.)	V_{33} (a.u.)
α-glycine	−0.0573	−0.1980	0.2553	−0.0491	−0.261	0.2552
β-glycine	−0.1280	−0.2114	0.3394	−0.0629	−0.2104	0.2733
γ-glycine	−0.0765	−0.1890	0.2655	−0.0771	−0.1858	0.2629
glycine HCl	−0.1039	−0.1448	0.2488	−0.0919	−0.1453	0.2372

Table S9. Statistically calculated CP enhancement for glycine HCl based on five spikelets.

Spikelet frequency (MHz)	DE S/N (au)	BCP S/N (au)	CP enhancement (BCP S/N ÷ DE S/N)
29.193995	46.9	299.7	6.39
29.213999	44.1	293.2	6.65
29.233987	56.5	379.3	6.71
29.253992	47.0	318.0	6.76
29.2739966	35.7	242.8	6.80
		average:	6.66 ± 0.16

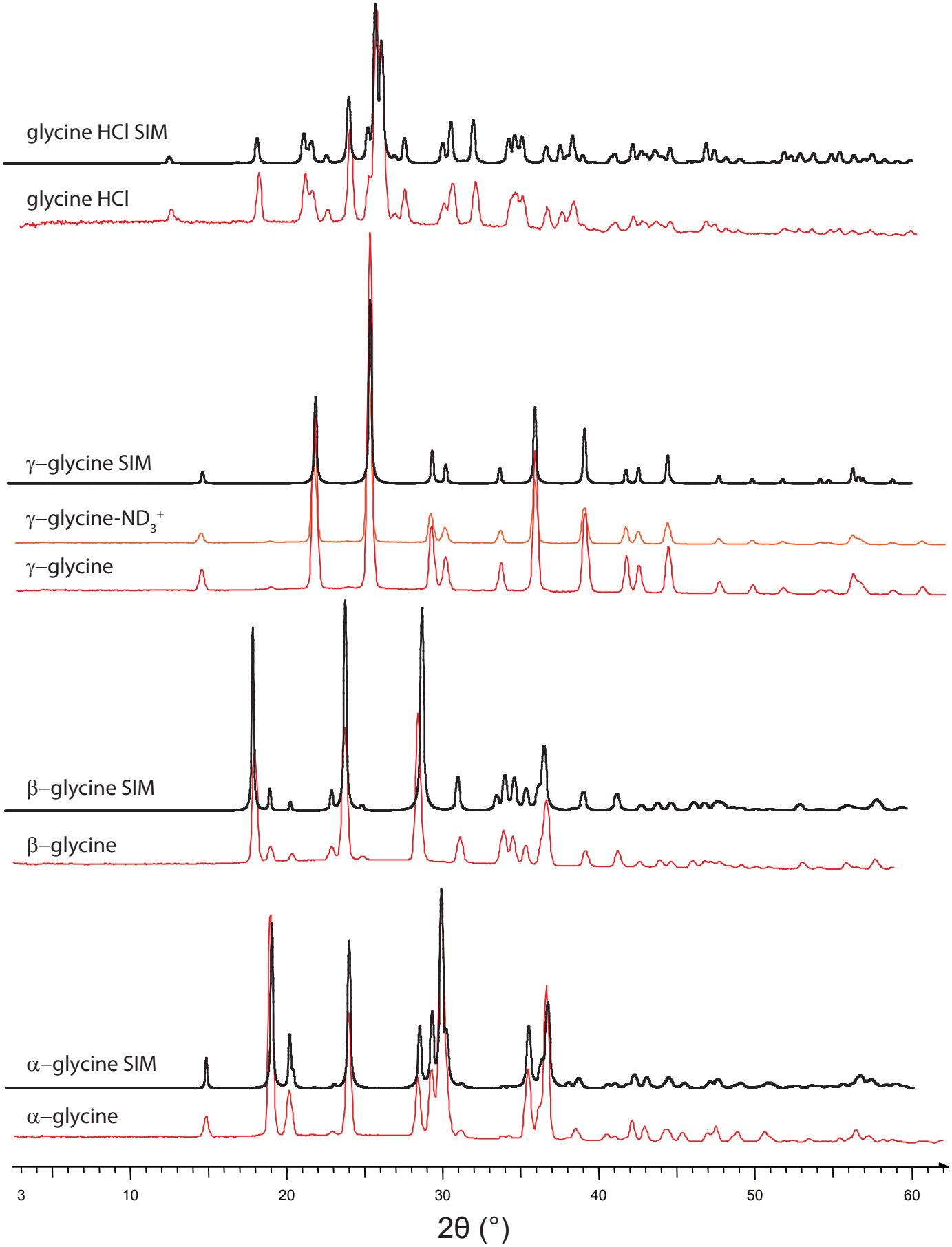

Figure S1. Powder X-ray Diffraction (pXRD) patterns for the three polymorphic forms of glycine and its HCl salt (red) along with simulated patterns (black).

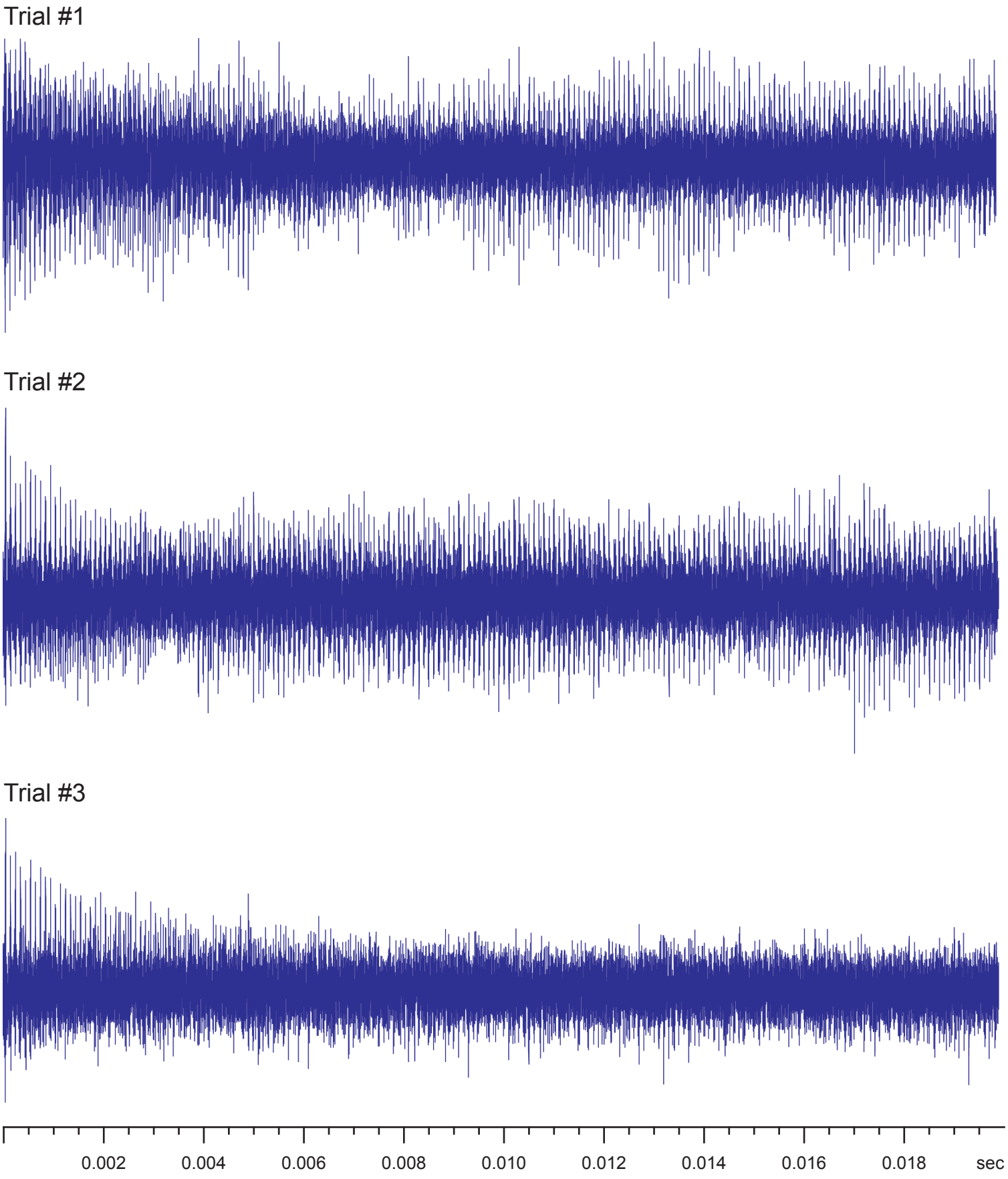

Figure S2. Severe acoustic ringing is observed in three individual ^{14}N FIDs of γ-glycine after 256 scans. All three trials were conducted with identical acquisiting parameters. The ringing is seen throughout the FIDs, is semi-coherent in nature, and is random in every scan. To minimize the contribution of the ringing to the FID, many acquisitions are required.

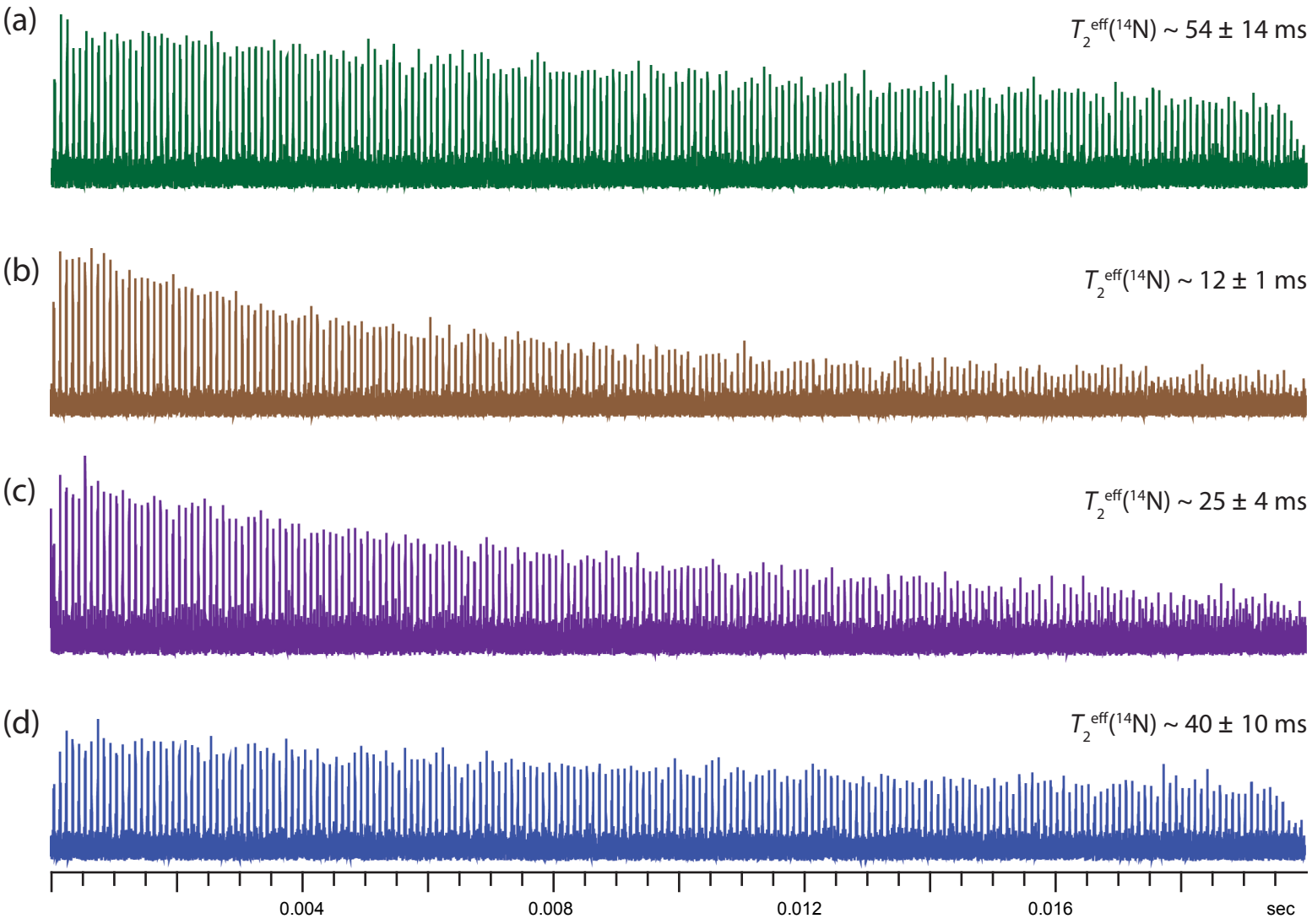

Figure S3. ^{14}N FIDs for (a) α-glycine, (b) β-glycine, (c) γ-glycine, and (d) glycine HCl after 256, 7200, 512, and 256 acquisitions, respectively. By fitting the FIDs with a first-order exponential decay function, the $T_2^{eff}(^{14}N)$ values for α-glycine, β-glycine, γ-glycine, and glycine HCl were determined to be 54 ± 14 ms, 12 ± 1 ms, 25 ± 4 ms, and 40 ± 10 ms, respectively.

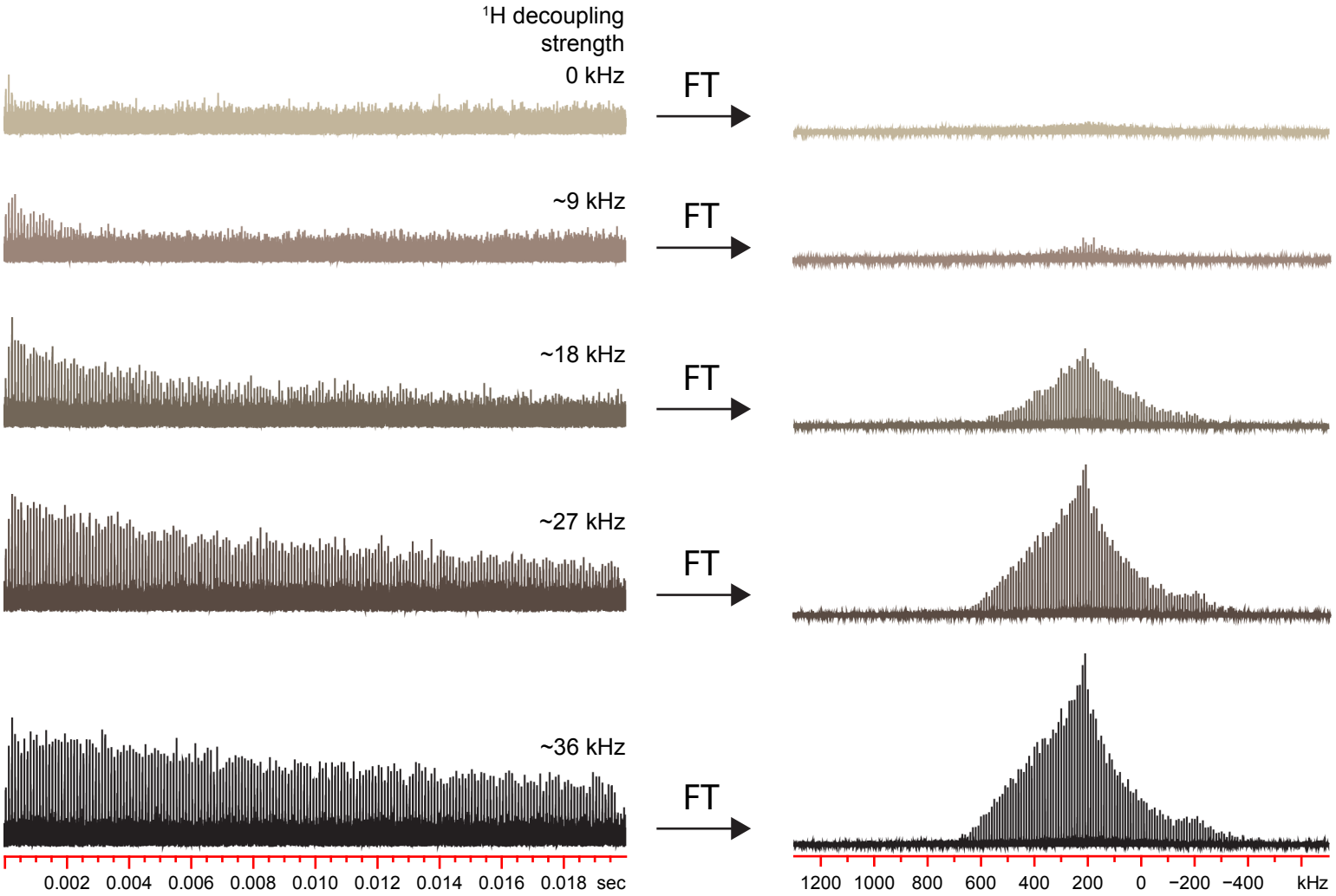

Figure S4. ^{14}N FIDs and corresponding FT NMR sub-spectra of α-glycine acquired at 29.175 MHz with varying ^{1}H decoupling rf field strengths. The number of spin echoes that form in the CPMG echo train, and their intensity, increases with increasing ^{1}H decoupling strength, resulting in FT NMR spectra with higher S/N.

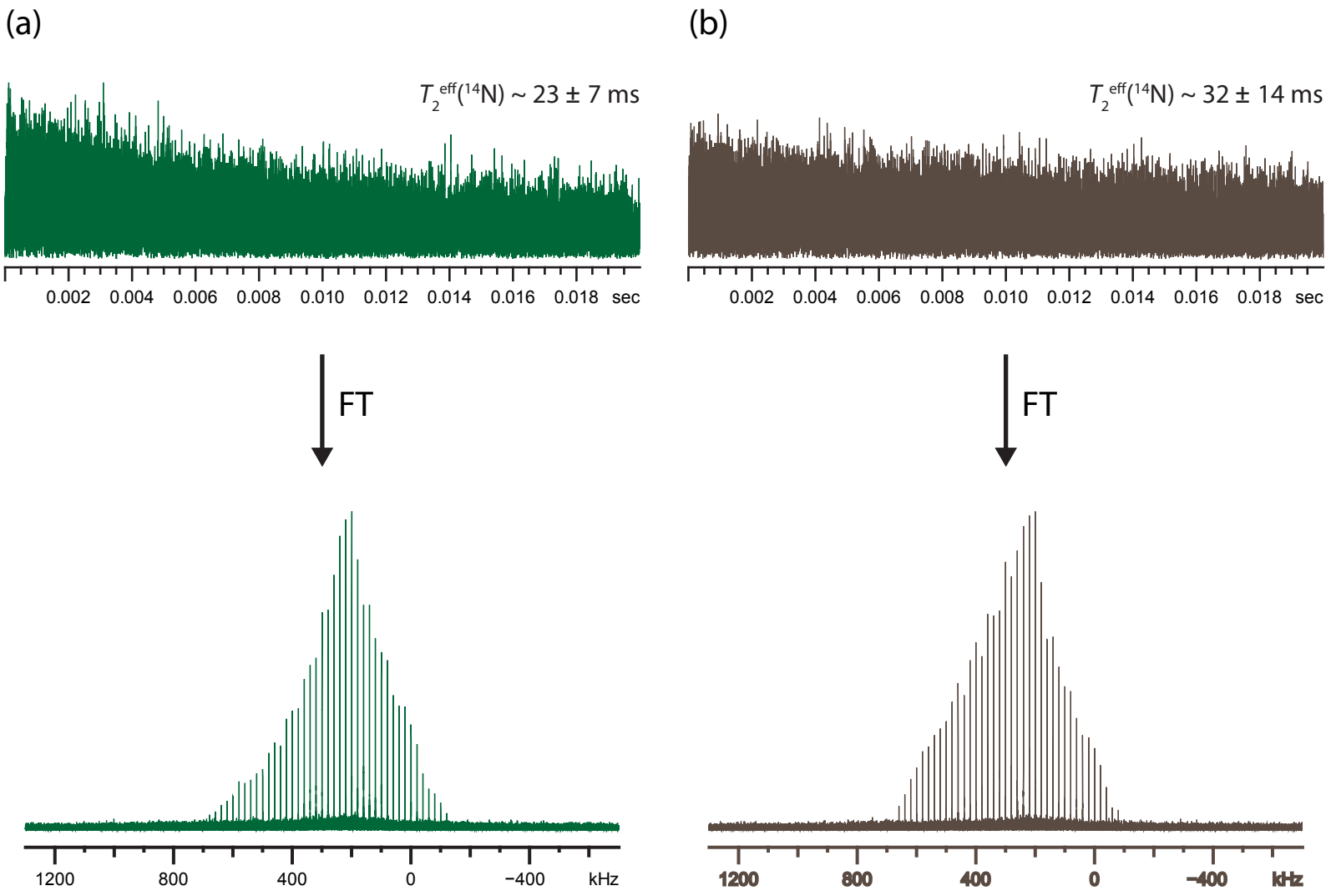

Figure S5. Comparison of ^{14}N FIDs and corresponding FT sub-spectra for (a) α-glycine and (b) α-glycine-D_5, acquired with the same experimental parameters. The $T_2^{eff}(^{14}N)$ values for α-glycine and α-glycine-D_5 were measured to be 23 ± 7 ms and 32 ± 14 ms, respectively. The high degree of uncertainty in the measurement of $T_2^{eff}(^{14}N)$ is a result of the low intensity of the individual spin-echoes in the FIDs.

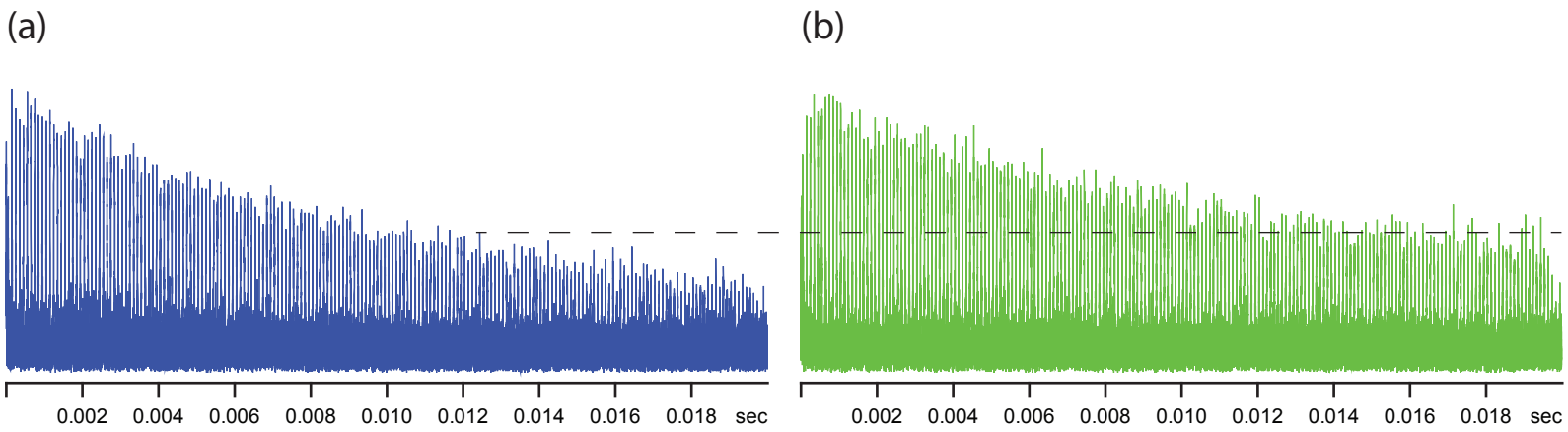

Figure S6. ^{14}N FIDs of γ-glycine acquired at sample temperatures of (a) 20 °C and (b) 92 °C. As evidenced by the horizontal dashed line, the intensity of the CPMG echo-train persists further in the time domain for the 92 °C FID. As a result, the corresponding Fourier-Transformed sub-spectrum at 92 °C has higher S/N than its 20 °C counterpart.

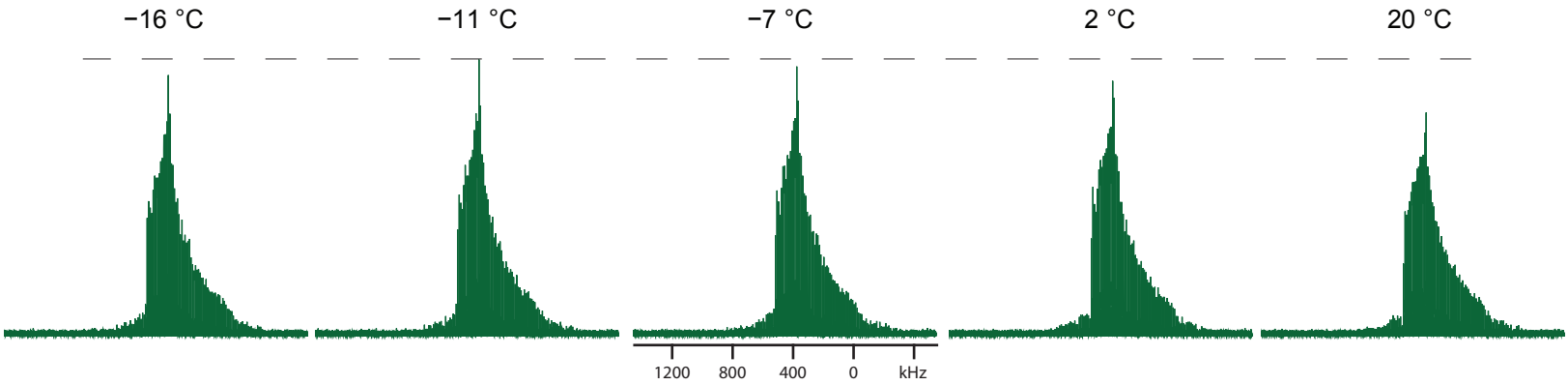

Figure S7. ^{14}N variable-temperature SSNMR of glycine HCl in the temperature range of −16 to 20 °C. The horizontal dashed line indicates the intensity of the ^{14}N sub-spectrum that has the highest S/N (T_{max} = −11 °C).

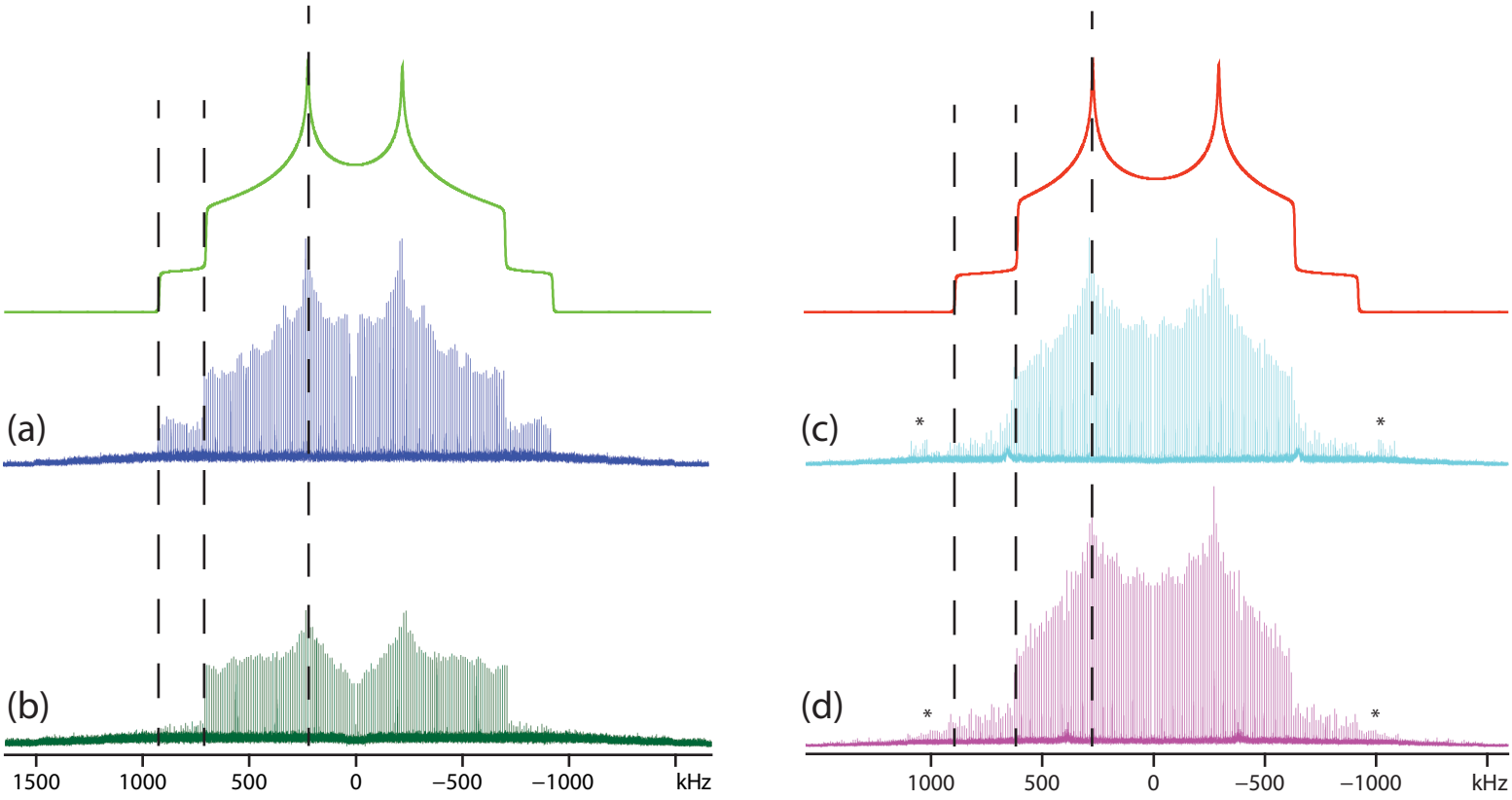

Figure S8. ^{14}N powder patterns of α-glycine at (a) 20 °C and (b) −42.7 °C and corresponding analytical simulation (green trace, C_Q = 1.22 ± 0.02 MHz and η_Q = 0.52 ± 0.02). Spectra of γ-glycine at (c) 20 °C and (d) 91.6 °C and corresponding analytical simulation (red trace, C_Q = 1.22 ± 0.04 MHz and η_Q = 0.38 ± 0.04). Relative positions of the discontinuities are shown by vertical dashed lines. * ^{14}N NMR signal arising from piezoelectric response of sample due to RF irradiation.